



# Approaches to Biomass Kinetic Modelling: Thermochemical Biomass Conversion Processes

Omar Al-Ayed<sup>\*</sup>, Walaa Saadeh

Chemical Engineering Department Faculty of Engineering Technology, Al-Balqa Applied University, P. O. Box 15008, 11134 Jordan.

## Abstract

Modeling of biomass pyrolysis kinetics is an essential step towards reactors design for energy production. Determination of the activation energy, frequency factor, and order of the reaction is necessary for the design procedure. Coats and Redfern's work using the TGA data to estimate these parameters was the cornerstone for modeling. There are two significant problems with biomass modeling, the first is the determination of the kinetic triplet (Activation energy, Frequency factor, and the order of reaction), and the second is the quantitative analysis of products distribution. Methods used in modeling are either One-step or Multistep methods. The one-step techniques allow the determination of kinetic triplet but fail to predict the product distribution, whereas multistep processes indicate the product's distribution but challenging to estimate the parameters. Kissinger, Coats, and Redfern, KAS, FWO, Friedman are one-step methods that have been used to estimate the kinetic parameters. In this work, after testing more than 500 data points accessed from different literature sources for coal, oil shale, solid materials, and biomass pyrolysis using one-step global method, it was found that the activation energy generated by KAS or FWO methods are related as in the following equations:  $E_{KAS} = 0.9629 * E_{FWO} + 8.85$ , with  $R^2 = 0.9945$  or  $E_{FWO} = 1.0328 * E_{KAS} - 8.0969$  with  $R^2 = 0.9945$ . The multistep kinetic models employed the Distributed Activation Energy Model (DAEM) using Gaussian distribution, which suffers from symmetry, other distributions such as Weibull, and logistic has been used. These multistep kinetic models account for parallel/series and complex, primary and secondary biomass reactions by force-fitting the activation energy values. The frequency factor is assumed constant for the whole range of activation energy. Network models have been used to account for heat and mass transfer (diffusional effects), where the one-step and multistep could not account for these limitations. Three network models are available, the Bio-CPD (Chemical Percolation Devolatilization) model, Bio-FLASHCHAIN, and the Bio-FG-DVC (Functional Group Depolymerization Vaporization Crosslinking models). These models tried to predict the product distributions of the biomass pyrolysis process.

**Paper type:** Research paper

**Keywords:** Biomass, Energy conversion, kinetics modeling, environment, clean energy.

**Citation:** Omar A., and Saadeh W. "Approaches to Biomass Kinetic Modelling: Thermochemical Biomass Conversion Processes", *Jordanian Journal of Engineering and Chemical Industries*, Vol.4, No.1, pp: 1-13, (2021).

## Introduction

Thermal decomposition reactions of biomass play a crucial role in its utilization processes (Balan, 2014). Biomass, which covers from tiny grass to massive trees and from animal waste to small insets (Basu, 2010), is a renewable energy source that produces heat and energy whenever needed (Anca-Couce, 2016; McKendry, 2002). Biofuels contain various pyrolyzing species with different reactivity and are probably influenced by surrounding species (Carpenter *et al.*, 2014). Biomass, by enlarge, comprises cellulose, which constitutes 38 – 50% of the total mass, hemicellulose, 20–32%, lignin 15–25%, and 5–13% other inorganic and extractive species (Hameed *et al.*, 2019). There are three principal routes to release heat and energy from biomass: Pyrolysis, direct combustion, and gasification (Cuoci *et al.*, 2007). The transformation of biomass can be performed either by biochemical or thermochemical methods. In biochemical conversion, sugar platform biorefinery includes physicochemical pretreatment of the biomass, the enzymatic hydrolysis of the carbohydrates to a fermentable sugar stream, and finally, the fermentation of the sugars by suitable microorganisms to the desired molecules (Simone and Michael, 2015).

\* Corresponding author: E-mail: [omar.alayed@bau.edu.jo](mailto:omar.alayed@bau.edu.jo)

Received on October 17, 2020;

*Jordanian Journal of Engineering and Chemical Industries* (JJECI), Vol.4, No.1, 2021, pp. 1-13.

ORCID: <https://orcid.org/0000-0002-0124-7449>.

Accepted on December 18, 2020.



The main thermochemical processes are gasification, pyrolysis, combustion, hydrothermal liquefaction, and hydrothermal carbonization (Behrendt *et al.*, 2008; Funke *et al.*, 2010; Basu, 2010; Sharma *et al.*, 2015). Processes that convert biomass into liquid fuels and other products proceed via the pyrolysis route.

The pyrolyzed bio-oil might undergoes upgrading (Zhang *et al.*, 2007; Demirbas, 2003a, 2003b) to improve properties and meet the end-user specifications. The kinetics of thermochemical pyrolysis is the essence of reaction rate, product distribution, and reactor design. Biomass pyrolysis is the process that is positively affected by a variety of parameters such as heating rate (Mishra and Mohanty, 2018), temperature (Angin Dilek, 2013), gas flow rate (Tripathi, *et al.*, 2016), biomass composition, residence time, moisture content, particle size (Koufopoulos *et al.*, 1989(a) 1991(b); Sheth and Babu, 2006; Ranzi, *et al.*, 2008; Vinu and Broadbelt, 2012), and type of reactor (Lédé, 2012). The importance of biomass pyrolysis kinetics is emanated from the need for gasifiers and combustors reactors design (Patra and Sheth, 2015). Design and optimization of reactors require estimating the relevant parameters such as activation energy, frequency factor, and reaction order that pertain to the decomposition process (Huang *et al.*, 2013; Meng *et al.*, 2013).

Numerous factors affect the pyrolysis rate, the yields, composition, and properties of the product classes. Temperature, pressure and heating rate, heating time (Gronli and Melaaen, 2000) affect the pyrolysis product distribution and are the main operating parameters (Newalkar *et al.*, 2014). In addition, biomass properties (chemical composition, ash content, composition, particle size and shape, density, moisture content (Demirbas, 2004; Mehrabian, *et al.*, 2012), heating value, *etc.*) also play an essential role.

Pyrolysis involves a breakdown of large complex molecules of the biomass into several smaller molecules. The cellulose, hemicellulose, and lignin undergo pyrolysis differently, contributing to yields. Hemicellulose, which is a short branched high molecular weight linear polymer of  $\beta$ -(1 $\rightarrow$ 4)-D-glucopyranose units of different monosaccharides linked to each other by (1-4)-glycosidic bonds (Mohan *et al.*, 2006) undergoes exothermic pyrolysis at temperatures between 150–350°C then, shifts to endothermic pyrolysis at higher temperatures (Broido and Nelson, 1975). Pyrolysis of hemicellulose yields more noncondensable gases such as CO<sub>2</sub>, CO, H<sub>2</sub>, CH<sub>4</sub>, C<sub>2</sub>H<sub>2</sub>, C<sub>2</sub>H<sub>4</sub>, C<sub>2</sub>H<sub>6</sub>. In addition to bio-oil and char. Cellulose is made of unbranched fibrils composed exclusively of glucose. Thermal destruction of cellulose during pyrolysis proceeds through gradual degradation, decomposition, and char formation at slow heating and low reaction temperatures. Rapid volatilization is accompanied by levoglucosan formation at high pyrolysis temperature and fast heating rates. The endothermic cellulosic degradation reactions occur in the range of 275–350°C; while exothermic reactions take place at higher temperatures. Cellulosic reactions include hydrolysis, depolymerization, oxidation, decarboxylation, and dehydration. The main liquid products are levoglucosan-pyranose, glycolaldehyde, formic acid, anhydrous xylopyranose, 5-hydroxymethyl furfural, and 2-furaldehyde, *etc.* (Patwardhan *et al.*, 2009) in addition to char and gaseous products. Lignin is a high molecular weight amorphous, a phenolic compound with different alcohol building units such as sinapyl, coniferyl, and p-coumaryl. Pyrolysis of lignin proceeds mainly in the temperature range between 200 and 500°C (Hosoya *et al.*, 2008). The pyrolysis of lignin culminated in the production of unsaturated side-chains, including alcohol, aldehyde, guaiacol, stilbene, gases, char.

There are a numerous studies on biomass pyrolysis kinetics for developing various kinetic models (Hameed *et al.*, 2019; Lam *et al.*, 2012; Hu *et al.*, 2007). Most pyrolysis kinetic models of biomass are considered lumped models since the kinetics are based on the yield of lumped products (*i.e.*, gas, bio-oil, and solid-char). More light will be shed on the different modeling kinetics and review mathematical development in this research work.

## 1 Materials and Methods

### 1.1 Chemical Aspects

#### 1.1.1 Mechanism and reaction modeling

Each of the structural constituents of biomass (cellulose, hemicelluloses, lignin, and extractives) is known to pyrolyze at different rates and by different mechanisms and pathways at various temperatures. These reactions are spread widely over the 150–550°C temperature range. The rates of reactions and extent of degradation of each of these reacting components depend on the process parameters, temperature, biomass type, particle size, heating input rate, and total pressure of the system. Bradbury *et al.*, 1979, studied cellulose pyrolysis and reported series (incubation period to convert inert materials to active components) and parallel reactions in which the first stage reactions were characterized by high activation energy. The pyrolysis products are gases of similar elements with a different distribution, liquids of varying structure and types, and char solids of other formats. (Chen, *et al.*, 2019; Yang *et al.*, 2007; Kawamoto, 2017). Chemical kinetics play a vital role in elucidating the characteristics of pyrolysis reactions and developing mathematical models needed for reactor design.

The early use of thermogravimetric data (TG) to evaluate kinetic parameters of solid-state reactions was used by Coats and Redfern in 1964. These authors advocated using a small size sample to eliminate the heat effect due to endo- or exothermic heat of reactions and maintain a linear heating rate and accurate temperature measurement.

It is stated that for solid-state chemical reactions, the rate of decomposition of reactant is proportional to its unreacted concentration and reaction temperature, as described in equation (1):

$$\frac{d\alpha}{dt} = kf(\alpha) = k(1 - \alpha)^n \quad (1)$$

where  $\alpha$  is the fraction of solid materials decomposed defined as indicated in equation (2) at any  $t$ ,  $n$  is the reaction order,

$$\alpha = (w_o - w_t)/(w_o - w_f) \quad (2)$$

where  $w_o$  is the initial weight of biomass,  $w_t$  is the weight of biomass at any run time,  $t$  and  $w_f$  is the final weight of biomass at the end of the run,  $k$  is the rate constant given by Arrhenius equation (3):

$$k = k_o \exp(-E/RT) \quad (3)$$

in which  $k_o$  is the frequency factor ( $s^{-1}$ ),  $E$  is the activation energy, ( $kJ/kmol$ ),  $R$  is the universal gas constant, ( $8.314 \text{ kJ//kmol K}$ ) and  $T$  is reaction temperature in ( $K$ ).

Introducing the linear heating rate,  $\beta = dT/dt$  into equation (1) to obtain equation (4)

$$d\alpha/dT = (k_o/\beta) \exp(-E/RT) (1 - \alpha)^n \quad (4)$$

If equation (4) is integrated, we obtain equation (5)

$$\int_0^\alpha \frac{d\alpha}{(1-\alpha)^n} = \frac{k_o}{\beta} \int_0^T \exp\left(-\frac{E}{RT}\right) dT \quad (5)$$

The RHS of equation (5) has no exact integral, but with some mathematical manipulations by substituting  $u = E/RT$  and using the relation of equation (6) (Coats and Redfern, 1964) to obtain equation (7) below:

$$\int_u^\infty \exp^{-u} u^{-b} du \approx u^{1-b} \exp^{-u} \sum_{n=0}^{\infty} \frac{(-1)^n (b)_n}{u^{n+1}} \quad (6)$$

Now, equation (5) becomes

$$\frac{1-(1-\alpha)^{1-n}}{1-n} = \frac{k_o RT^2}{\beta E} \left[1 - \frac{2RT}{E}\right] \exp\left(-\frac{E}{RT}\right) \quad (7)$$

If the logarithm of both sides is taken, we obtain equation (8) as follows

$$\ln \left\{ \frac{1-(1-\alpha)^{1-n}}{(1-n)T^2} \right\} = \ln \left( \frac{k_o R}{\beta E} \right) \left[1 - \frac{2RT}{E}\right] - \frac{E}{RT} \quad (8)$$

If reaction order in equation (5) is taken to be unity (a special case of equation (8)) and after taking the logarithm, equation (9) is obtained:

$$\ln \left[ \frac{-\ln(1-\alpha)}{T^2} \right] = \ln \frac{k_o R}{\beta E} \left[1 - \frac{2RT}{E}\right] - \frac{E}{RT} \quad (9)$$

Plotting the left hand side(LHS) of equation (9) against the inverse of reaction temperature ( $1/T$ ) would results in activation energy calculations from the slope of the straight line resulted from plotting the data. Simultaneously, the frequency factor could be determined from the intercept of the line with the y-axis. The quantity  $\ln \frac{k_o R}{\beta E} \left[1 - \frac{2RT}{E}\right]$  is assumed constant (Coats and Redfern, 1964).

Furthermore, the magnitude of the quantity  $2RT/E$  within the range of biomass reactions, temperatures are relatively small compared with unity. Hence, it could be neglected; as a result of both cases, the intercept would value the frequency factor. Equation (9) has been extended or modified and developed further to model solid-state decomposition reactions. In the present work, several kinetic models based on equation (9) will be discussed and used by investigators within the scope of biomass pyrolysis kinetic modeling. The majority of kinetic models used by researchers employed a one-step global kinetic model or more than one-step kinetic models such as parallel and competitive reactions. The detailed lumped kinetic model, models with secondary bio-oil cracking, distributed activation energy model (DAEM) based on Gaussian distribution (Braun and Burnham, 1987), Weibull (Lakshmanan and White, 1994) and Gamma distributions (William and Tarutis, 1994), and nucleation growth model. **Figure 1** shows the various kinetic models employed by investigators. As indicated, one-step and multistep models have been used.

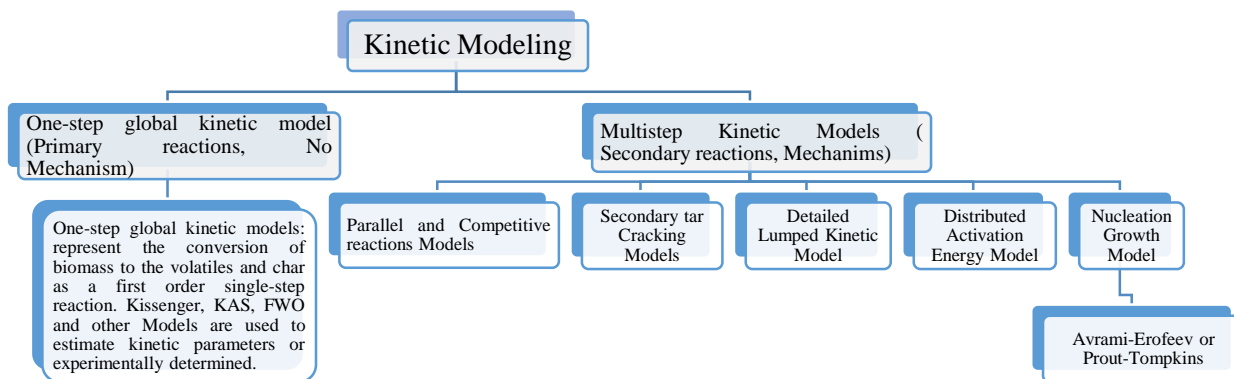


Fig. 1 Various kinetic models employed for biomass reactions.

## 1.2 Kinetic modeling

### 1.2.1 One-Step global kinetic model

The one-step global kinetic models represented by a first-order single-step reaction are the simplest pyrolysis models representing the conversion of biomass to the volatiles (vapors and non-condensable) solid-char. The pyrolysis products only consist of char and only volatiles (White *et al.*, 2011). This one-step kinetic model was also employed for intrinsic kinetics and under the influence of heat and mass transfer limitations (Antal *et al.*, 1998; Prakash and Karunanithi, 2008). These models do not account for the reaction mechanism concerned with immediate reactions for volatiles and solid-char as final products. Several models such as Kissinger Model, Flynn-Wall-Ozawa (FWO), Kissinger-Akahira Sunose (KAS), and Friedman, Coats, and Redfern have been developed and used (Papari and Hawboldt, 2015).

### 1.2.2 Kissinger model equation

The widely used Thermal Gravimetric Analysis/Differential Thermal Analysis (TGA/DTA) for conducting experimental work is a thermal analysis in which the reacted mass is measured as a function of time at non-isothermal conditions with a constant linear heating rate. When the DTA data are plotted against the pyrolysis temperature, the curve exhibits a maximum mass loss rate at a specific temperature. At a maximum rate of decomposition at the peak of DTA curve, the first derivative of equation (1) would be zero, and the corresponding temperature  $T_m$  is termed characteristic temperature. Taking the second derivative at constant linear heat rate  $\beta = dT/dt$  equation (10) is obtained as follows:

$$\frac{d}{dt} \left( \frac{d\alpha}{dt} \right) = \frac{d\alpha}{dt} \left( \frac{E}{RT_m^2} \frac{dT}{dt} + \frac{df(\alpha)}{d\alpha} k_o \exp \left( \frac{-E}{RT_m} \right) \right) \tag{10a}$$

$$\left( \frac{d\alpha}{dt} \right) \left[ \frac{E}{R T_m^2} \beta + \frac{df(\alpha_m)}{d\alpha} k_o \exp \left( \frac{-E}{RT_m} \right) \right] = 0 \tag{10b}$$

Since the rate of conversion, i.e.  $d\alpha/dt$  is a non-zero value, then the square bracket term must be zero leading to Kissinger’s equation (Kissinger, 1957) indicated as equation (11) in which after taking the logarithm and rearrangement becomes:

$$\ln \left( \frac{\beta}{T_m^2} \right) = \ln \left[ \frac{-k_o R}{E} \frac{df(\alpha_m)}{d\alpha} \right] - \frac{E}{RT_m} \tag{11}$$

If the reaction rate order is assumed unity, and for a given value of the linear heating rate  $\beta$ , equation (11) is employed to estimate the frequency factor and activation energy by plotting  $\left[ \ln \left( \frac{\beta}{T_m^2} \right) \right]$  against the inverse of several values of  $T_m$ .

### 1.2.3 Flynn-Wall-Ozawa (FWO) model equation

The right hand side (RHS) integral of equation (5) can be expressed through (Doyle, 1961) tabulated values as indicated in equation (12):

$$\frac{k_o}{\beta} \int_0^T \exp \left( -\frac{E}{RT} \right) dT = \frac{k_o E}{\beta R} p \left( \frac{E}{RT} \right) \tag{12}$$

If the quantity  $\left(\frac{E}{RT}\right)$  is larger than 20, the quantity  $p\left(\frac{E}{RT}\right)$ , can be approximated and become exact (Doyle, 1962) as in equation (13) which is obtained from the tables of the exponential values.

$$\log(E/RT) = -2.315 - 0.4567 E/RT \quad (13)$$

Whereas equation (13) becomes inexact if the quantity  $\left(\frac{E}{RT}\right)$ , is less than 20. Furthermore, equation (5), after introducing the approximation, becomes equation (14):

$$\int_0^\alpha \frac{d\alpha}{(1-\alpha)} = g(\alpha) = \frac{k_0}{\beta} \int_0^T \exp\left(-\frac{E}{RT}\right) dT = \frac{k_0 E}{\beta R} p\left(\frac{E}{RT}\right) = \left(\frac{E k_0}{\beta R}\right) \ln\left(\frac{E}{RT}\right) \quad (14a)$$

$$\ln[g(\alpha)] = \ln\left(\frac{E k_0}{\beta R}\right) - 2.315 - 0.4567 \frac{E}{RT} \quad (14b)$$

Rearranging:

$$\ln(\beta) = \ln\left(\frac{E k_0}{g(\alpha) R}\right) - 2.315 - 0.4567 \frac{E}{RT} \quad (14c)$$

Now, for any evolved biomass loss quantity, i.e. a given constant value of the conversion function,  $\alpha$ , the left-hand side of equation (14b) is independent of heating rate. Suppose the conversion function  $\alpha$  is kept constant for several heating rate values. In that case, the LHS plot of equation (14c) against the pyrolysis temperature inverse will culminate in activation energy and frequency factor determination. FWO method's advantage is that it does not require any form of kinetic model other than the Arrhenius equation for temperature dependence. The FWO method is a model-free that involves measuring the temperatures corresponding to fixed values of conversion function  $\alpha$  from experiments at different heating rates,  $\beta$ .

### 1.2.3 Kissinger-Akahira Sunose (KAS)

The KAS method is based on equation (5) with the approximation in equation (6) to obtain equation (15)

$$\int_0^\alpha \frac{d\alpha}{f(\alpha)} = \frac{k_0}{\beta} \int_0^T \exp\left(-\frac{E}{RT}\right) dT = \frac{k_0 R T^2}{\beta E} \left[1 - \frac{2RT}{E}\right] \exp\left(-\frac{E}{RT}\right) \quad (15)$$

and if the quantity  $\frac{2RT}{E}$  is  $\ll 1$ , then equation (15) can be written as indicated by equation (16) i.e.

$$\int_0^\alpha \frac{d\alpha}{f(\alpha)} = g(\alpha) = \frac{k_0 R T^2}{\beta E} \exp\left(-\frac{E}{RT}\right) \quad (16a)$$

Rearranged after taking the logarithm of both sides:

$$\ln\left(\frac{\beta}{T^2}\right) = \ln\left(\frac{R k_0}{g(\alpha) E}\right) - \frac{E}{RT} \quad (16b)$$

The activation energy and frequency factor are determined if the LHS of equation (16b) is plotted against the inverse of pyrolysis temperature for several values of the heating rate at a constant conversion function  $g(\alpha)$  value. The difference between KAS and FWO is the method of evaluating and approximating the value of the integral of  $\left(\int_0^T \exp\left(-\frac{E}{RT}\right) dT\right)$ . Figure 2 shows the direct relationship between the activation energy obtained through KAS method and the activation energy estimated using FWO method. The closeness of the values predicted by both ways is related to the methodology of approximating the RHS, i.e. the integral part of the equation (15). The presented data in Fig. 2 are sourced from different studies and arbitrarily selected (more than 28 references) investigation of biomass, lignite coal and oil shale pyrolysis studies (Aboulkas and El-Harfi, 2008; Zou *et al.*, 2010; Damartzis *et al.*, 2011; Al-Ayed, 2011; Katarzyna *et al.*, 2012; Mishra and Bhaskar, 2014; Kongkaew *et al.*, 2015; Heydari *et al.*, 2015; Islam *et al.*, 2015; Maurya *et al.*, 2016; Ahmad *et al.*, 2017; Chandrasekaran *et al.*, 2017; Mishra and Mohanty, 2018; Xu Bang *et al.*, 2018). As it can be inferred from the plots, **Figure 2** and **Figure 3**, the activation energies estimated by KAS and FWO methods are related as indicated by equation (16). Equation (16a) predicts the KAS estimated activation energy as a function of the FWO calculated activation energy. Equation (17) is generated from actual experimental data taken from the pyrolysis of different biomass, coal, oil shale, and solid material reactions.

$$E_{KAS} = 0.9629 * E_{FWO} + 8.85, R^2=0.9945 \quad (17a)$$

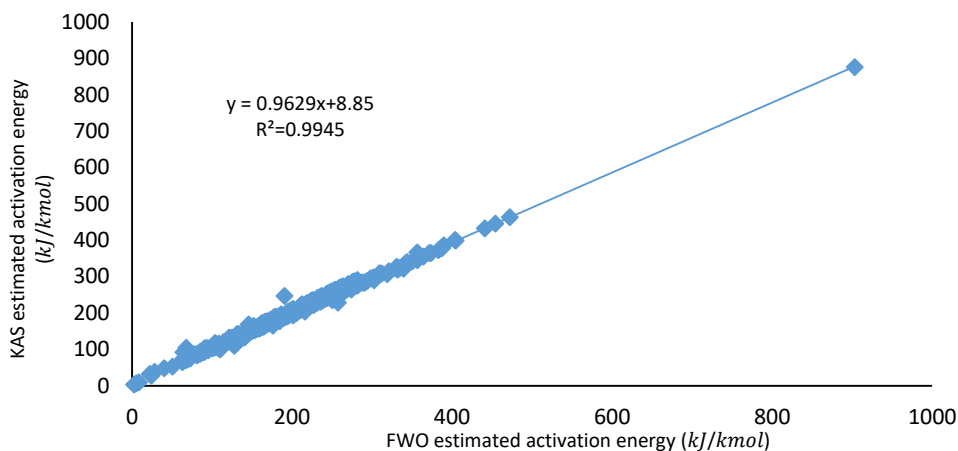


**Fig. 2** Comparison of the activation energies obtained for KAS and FWO methods from different literature. (sources: Mishra, et al., 2018 and refs. from Aboulkas and El-Harfi, 2008 until Chen et al., 2015)

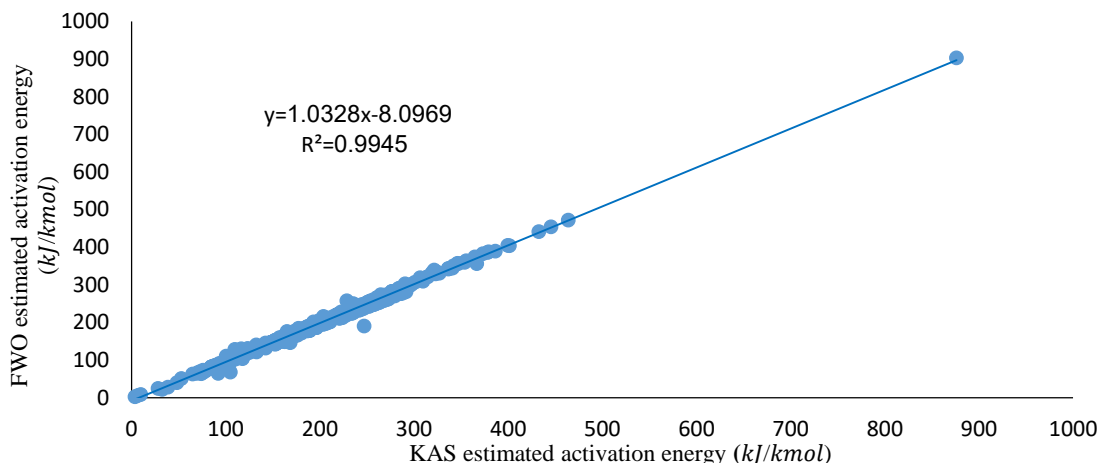


**Fig. 3** Comparison of the activation energies obtained for KAS and FWO methods from different literature sources. (sources: Mishra, et al., 2018 and refs. from: Aboulkas and El-Harfi, (2008) until Chen et al., 2015)

When the plotted data are exchanged on the axis, the FWO estimated activation energy is given as a function of KAS estimated activation energy as indicated in equation (17); it is worth noting that this equation is generated through trend line of the data plotted on Fig. 3 rather than a rearrangement of equation (17a).

$$E_{FWO} = 1.0328 * E_{KAS} - 8.0969, R^2=0.9945 \tag{17b}$$

The coefficient of determination  $R^2$  the value which measures the goodness of the fit, is relatively high, indicating an excellent correlation between the KAS and FWO methods of predicted activation energies. Coefficients of equation (17) could be improved furthermore if more published data are included in the plot to become universal, although more than 500 data points have been used to plot Fig. 2 and 3. It is quite possible to generate the KAS activation energy values from the corresponding FWO calculated energy values and vice-versa for any biomass, coal, oil shale, and any other solid material without conducting actual calculations. It can be concluded that KAS method is basically the same as FWO method and vice-versa since the small difference between the results inferred between both ways is related to the approximation procedure. This newly obtained equation (17) can replace the process of calculating the activation energy of either KAS or FWO calculations work if either of the pertaining values of KAS or FWO are calculated from the experimentally found data. Also, the generated equation could be used to create a check value on the experimentally determined activation energy. It should be noted that equations (17a) and (17b) are obtained directly from plotting data.

### 1.2.4 Friedman method

The un-widely used power-law method of Friedman (Friedman, 1960) is a technique for obtaining kinetic parameters that describe the thermal degradation using TGA data. This is a differential isoconversional method where it is possible to determine the activation energy of specific processes without knowing the kinetic equation. If the logarithm of both sides of equation (1) is taken, equation (18) is obtained as follows:

$$\ln\left(\frac{d\alpha}{dt}\right) = -\frac{E}{RT} + \ln(k_0 f(\alpha)^n) \quad (18)$$

In this method, the conversion functions  $f(\alpha)$  is assumed constant, indicating that biomass decomposition is independent of reaction temperature and depends only on the mass rate loss. Friedman believed that there was a single value of the reaction order ( $n$ ), which indicates that the value of  $E/R$  is the same for all levels of conversion. A plot of the LHS of equation (18) against the inverse of pyrolysis temperature would lead to the activation energy. However, the slope's actual value is not the same for all conversion levels (Mishra and Mohanty, 2018). Different forms of the conversion function are assumed, as shown in table 1.

### 1.2.5 Coats-Redfern method

The Coats-Redfern equation is an integral model-free method (Coats and Redfern, 1964), broadly used to calculate reaction order and pre-exponential factor (Damartzis *et al.*, 2011). Equation (7) can be rewritten as in equation (18)

$$g(\alpha) = \int_0^\alpha \frac{d\alpha}{f(\alpha)} = \frac{k_0 RT^2}{\beta E} \left[ 1 - \frac{2RT}{E} \right] \exp\left(-\frac{E}{RT}\right) \quad (19)$$

Using an asymptotic approximation for the resolution of Eqn. (19) and if  $(2RT/E \ll 1)$ , equation (20) can be obtained:

$$\ln\left(\frac{g(\alpha)}{T^2}\right) = \ln\left(\frac{Rk_0}{\beta E}\right) - \frac{E}{RT} \quad (20)$$

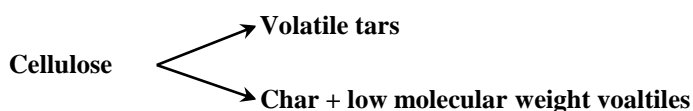
If equation (20) is compared with equation (16b), we note both equations are the same except exchanging the location of the quantity  $g(\alpha)$  with that of the heating rate,  $\beta$ . It is concluded that the three methods, namely, KAS, FWO, and Coats and Redfern, are basically the same, and the only difference is the type of model used in the Coats and Redfern equation. In other words, KAS method is a particular case of the Coats and Redfern equation since several models (in addition to reactants nature and composition, pyrolysis products distribution influenced by the operating conditions during the reaction) can be used to find the  $g(\alpha)$  as indicated in **Table 1**.

**Table 1** List of reaction models used by researchers.

Reaction Model	Symbol	$f(\alpha)$	$g(\alpha)$
Power law	$p^{\frac{1}{4}}$	$4\alpha^{3/4}$	$\frac{1}{3}\alpha^{1/4}$
Power law $n=\frac{1}{3}$	$p^{\frac{1}{3}}$	$3\alpha^{\frac{2}{3}}$	$2\alpha^{-\frac{1}{3}}$
Power law $n=\frac{1}{2}$	$p^{\frac{1}{2}}$	$2\alpha^{\frac{1}{2}}$	$a^{-\frac{1}{2}}$
Power law $n=\frac{3}{2}$	$p^{\frac{3}{2}}$	$\frac{2}{3}\alpha^{-\frac{1}{2}}$	$-\frac{1}{3} * a^{-\frac{3}{2}}$
One-D diffusion (Parabola law)	$D^1$	$\frac{1}{2}\alpha^{-1}$	$-\frac{1}{2}\alpha^{-2}$
Mampel ( $n = 1$ )	$F^1$	$1 - a$	$-1$
Mampel ( $n^{th}$ order)	$F^n$	$(1 - a)^n$	$-n(1 - a)^{n-1}$
Avrami-erofeev ( $n = 4$ )	$A^4$	$4(1 - a)(-\ln(1 - a))^{\frac{3}{4}}$	$(4 \ln(1 - a) + 3)(-\ln(1 - a))^{-\frac{1}{4}}$
Avrami-erofeev ( $n = 3$ )	$A^3$	$3(1 - a)(-\ln(1 - a))^{\frac{2}{3}}$	$-(3 \ln(1 - a) + 2)(\ln(1 - a))^{-\frac{1}{3}}$
Avrami-erofeev ( $n = 2$ )	$A^2$	$2(1 - a)(-\ln(1 - a))^{\frac{1}{2}}$	$(2 \ln(1 - a) + 1)(-\ln(1 - a))^{-\frac{1}{2}}$
3-D (Jander model)	$D^3$	$\frac{3}{2}(1 - a)^{\frac{3}{2}}(1 - (1 - a)^{\frac{1}{3}})^{-1}$	$\frac{1}{2}((1 - a)^{\frac{1}{3}} - 2)((1 - a)^{\frac{1}{3}} - 1)^{-2}(1 - a)^{-1/3}$
Contracting sphere	$R^3$	$3(1 - a)^{\frac{2}{3}}$	$-2(1 - a)^{-\frac{1}{3}}$
Contracting cylinder	$R^2$	$2(1 - a)^{\frac{1}{2}}$	$-(1 - a)^{-\frac{1}{2}}$
2-D diffusion (Valensi model)	$D^2$	$(-\ln(1 - a))^{-1}$	$(-\ln(1 - a))^{-2}(a - 1)^{-1}$

### 1.2.6 Multistep kinetic models (secondary reactions mechanism)

The one-step global kinetic models represent the characteristics of the simple biomass conversion to gas, bio-oil, and char; it does not account for or consider the nature of the biomass, the constituents, the reaction operating conditions such as pressure, liquid hourly space velocity, rate of heat input, thermodynamics, etc. The simple one-step global kinetic models are used to estimate the kinetic parameters for immediate reactions but did not tackle the kinetics of secondary reactions that takes place in parallel/series or an elaborate manner after the initial decomposition of the biomass (Vinu and Broadbelt, 2012; Corbetta *et al.*, 2013). The one-step global kinetic model's main advantages are the ease and direct determination of the activation energy, the frequency factor, and the needless of the reaction mechanism, and the disadvantage is the inability to predict the product's composition distribution. As a result, it is imperative to search for models that could predict product distribution, including primary and secondary biomass pyrolysis processes. Researchers formulated models to include the primary' reactions products as secondary reactions to produces materials similar to the direct products, i.e., gas, tar, and char, through cracking and polymerization reactions (Turner, 1981; Bradbury, *et al.*, 1979; Scott, *et al.*, 1985; Agrawal, 1988). Several kinetic schemes have been proposed for combining primary degradation of biomass and secondary decomposition of volatile products (higher molecular weight hydrocarbons). As early as 1975, Broido and Nelson formulated a multistep kinetic model by lumping the consecutive steps of cellulose reaction into a single, overall, first-order reaction as follows:



Broido and Nelson's model was further reformulated (Bradbury *et al.*, 1979) to include a cellulose activation reaction (incubation period). The cellulose is catalyzed through temperature treatment to initiate the reaction shown in **Figure 4**. The proposed scheme is presented as follows:

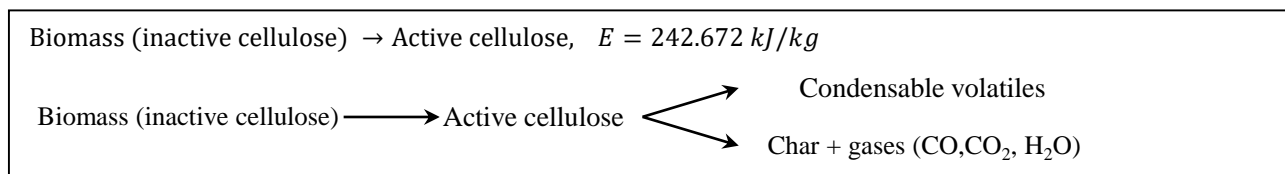


**Fig. 4** Bradbury and coworkers model of cellulose reaction.

The model developed by Bradbury and coworkers (Bradbury *et al.*, 1979) was further modified (Diebold, 1994) to consist of several intermediate and secondary reactions, as indicated in **Figure 5**.

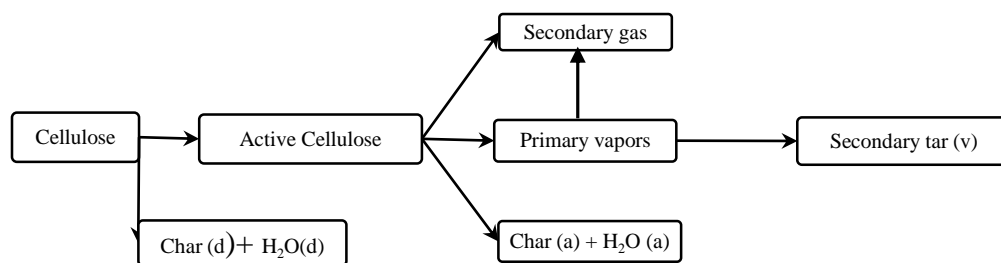


**Fig. 5** Seven global reaction scheme for cellulose pyrolysis.

Shafizadeh and Bradbury's model included both primary biomass pyrolysis reactions and secondary tar decomposition. In this model, (Bradbury *et al.*, 1979), cellulose was first converted to an intermediate component (active cellulose), which is further decomposed to other secondary products. Furthermore, they assumed an initiation reaction for the cellulose to be functional (incubation period) in which no weight loss is observed. The apparent activation energy was estimated as 424.67kJ/kg. Two competitive first-order primary reactions to produce condensable volatiles and char cum gases ( $\text{H}_2\text{O}$ ,  $\text{CO}$ , and  $\text{CO}_2$ ) were assumed to take place. The proposed model gave good predictions for the product yield (Di Blasi, 2008), but kinetic parameters' determination was difficult. Researchers have used this model in its original form and extended formulation (Sheth and Babu, 2006; Varhegyi *et al.*, 1994).

Kinetic models characterizing the main structures of devolatilization of the three components of the biomass have been developed by Cuoci and coworkers (Cuoci *et al.*, 2007). Complete prediction of product and by-product has been reported based on a semi-detailed kinetic mechanism. This proposed mechanism included 15 reactions with 30 lumped product species. The development of Cuoci *et al.*, was extended by Ranzi and associates (Ranzi *et al.*, 2008) to a mechanistic model to describe the biomass pyrolysis, devolatilization, and gas-phase reaction of the product gas species from cellulose, hemicellulose, and lignin of the biomass. Other researchers (Corbetta *et al.*, 2013) extended the works of Ranzi *et al.*, to encompass gas-phase secondary reactions; further extension of this work was conducted (Couce *et al.*, 2014) to include secondary char formation reactions under diffusional influences and in the absence of ash-alkali-metals effect to avoid sugar formation. It can be concluded from the published literature that all proposed mechanisms are the same if operating conditions such as temperature, pressure, and reaction environment, the residence time of products, biomass particle size, slow/fast heating rate, biomass constituents, and nature are alienated from influencing the biomass reactions. **Figure 6** shows the different proposed mechanisms and the progress of suggested decomposition, depolymerization chemical reactions, and effect of reaction products.

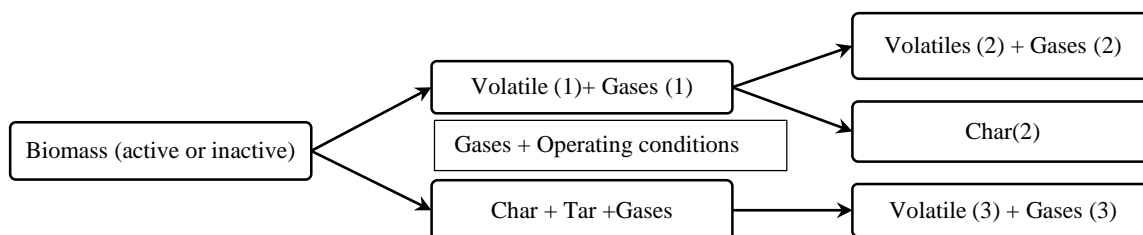


**Fig. 6** Pyrolysis reactions and product variations (Varhegyi *et al.*, 1997; Sheth and Babu, 2006; Ranzi *et al.*, 2008).

During pyrolysis, the operating conditions, such as fast or low heating rate, could produce more or less tar than char (Klass, 1998). Fast heating yields higher volatiles and reactive char than the slow heating process (Basu, 2010). In contrast, slow heating with longer residence time produces more char due to secondary reaction between formed char and volatiles (De Groot and Shafizadeh, 1984). The Distribution of Activation Energy Model (DAEM) has been recently used to understand the pyrolysis process complexity. The DAEM considers many primary and secondary biomass independent reactions with the activation energy for each reaction estimated by the Gaussian distribution continuous function (Hu *et al.*, 2016). Soria-Verdugo *et al.*, (2014) found a difference between the activation energies and frequency factors calculated at low and high heating rates during the TGA tests. DAEM was used to model municipal solid waste and agricultural residues pyrolysis at low heating rates using non-isothermal TGA analysis (Bhavanam and Sastry, 2015). The DAEM could model and explain the devolatilization curve for microalgae pyrolysis (Ceylan and Kazan, 2015). A three pseudo-components DAEM was developed using probability density function (PDF) to describe the biomass conversion and thermal decomposition rates during *Rhus Typhina* pyrolysis (Liu *et al.*, 2019).

The Gaussian distribution disadvantage is that it is symmetric, whereas the real reactivity distributions are asymmetric (Burnham and Braun, 1999). The asymmetry can be accounted for using other distributions, e.g., the Weibull (Lakshmanan and White, 1994) or Logistic distributions (Cai *et al.*, 2011a, b). These models, multistep and one-step global kinetics, have been employing TGA tests and did not account for the mass and heat transfer diffusional limitations. At higher heating rates or large biomass particle size, the effect of mass and heat transfer become predominant. All the lumped product models (gases, tar, and char) were not able to explain the complex biomass pyrolysis reactions and the formation of several species. Therefore, network models have been utilized to address these diffusional limitations (Hameed *et al.*, 2019).

### 1.2.7 Network models

Pyrolysis basically is a devolatilization process, which is a term for removing volatiles from solid materials such as coal, oil shale, and others. Devolatilization is similar to the desorption step in heterogeneous chemical reactions (catalytic reactions), i.e., one diffusional direction process (products desorption from inner of catalyst, reaction site to external surface of catalyst). Devolatilization generally involves reactions such as molecular-level depolymerization and polymerization (Wan *et al.*, 2015). As shown in **Figure 7**, the diffusional process steps are divided into four stages in series and are considered the main stages of the network models (Borah *et al.*, 2011).



Fig. 7 Stages of solid material reaction and diffusion of products to external surface in network models.

Researchers have developed three network models, which are also called structural models; the typical biomass network models are the Bio-CPD (Chemical Percolation Devolatilization) model (Sheng and Azevedo, 2002), the Bio-FLASHCHAIN model (Serio, 1997), and the Bio-FG-DVC (Functional Group Depolymerization Vaporization Crosslinking) model (Niksa, 2000). The bio-Chemical Percolation Devolatilization model (CPD) proposes that the solid materials are assumed to be clusters joined together through chemical bridges. Some of these connectors break at low temperatures, while others break at higher reaction temperatures. Low temperature breaking bridges give rise to gases and bio-oil (tar) formation, whereas those breaks at higher reaction temperatures give rise to char formation (Sheng and Azevedo, 2002). Workers (Lewis and Fletcher, 2013) predicted sawdust pyrolysis yields from a flat-flame burner using the CPD model. They assumed that the yield is the sum of the weighted average yield of the biomass's main components. Bio-FLASHCHAIN model was modified for biomass pyrolysis (Niksa, 2000) since initially it was developed for rapid coal pyrolysis. DISCHAIN, DISARAY, and FLASHTWO are the three concepts of the Bio-FLASHCHAIN theory. DISCHAIN concept is depolymerization, and cross-linking indicates the evolution of tar from the main reactant chains to small fragments; the produced monomers may react to the long pieces forming tar precursors by cross-linking to char, respectively. DISARAY is similar to DISCHAIN concept but applied to the two-dimensional structure. The FLASHTWO concept accounts for pressure effects, which has not been studied (Niksa, 1987).

The third structural FG-DVC model consists of two implicit models, responsible for forming light gases due to the decomposition of the biomass functional groups and the polymerization of fragments as time proceeds to form tar. The first FG model accounts for the Function Group, and the second is the DVC (Depolymerization, Volatilization, and the Cross-linking model or the tar-formation model (Solomon *et al.*, 1993). The DVC model determined the molecular weight distribution of char formed (Solomon and King, 1983).

## Conclusions

The one-step global method is widely and most popular model used by researchers for determining the kinetic parameters. The lumped model is a free kinetic model. Multistep kinetic models use different reaction mechanisms and consider primary and secondary biomass reactions to assess the kinetic parameter cumbersome. Distribution activation energy model using Gaussian and other distributions to estimate the kinetic parameters. Since none of the one-step and multistep models could account for the diffusional limitations, the network model could be more appropriate to address these issues. The one-step models such as KAS and FWO were successfully correlated in a single equation since both methods' difference lies in the approximation procedure for the same equation.

## Nomenclature

$A$	=Area	$[m^2]$
$C_p$	=Specific heat capacity	$[J/g.K]$
$k$	=Thermal conductivity	$[W/m.K]$
$L$	=Length	$[m]$
$m$	=Mass	$[g]$
$\alpha$	=Fraction of solid materials decomposed	$[-]$
$n$	=The reaction order	$[-]$
$w_o$	=Initial weight of biomass	$[g]$
$w_t$	=weight of biomass at any run time	$[g]$
$k$	=The rate constant	$[s^{-1}]$
$k_o$	=Frequency factor	$[s^{-1}]$
$E$	=The activation energy	$[kJ/kmol]$
$R$	=The universal gas constant	$[kJ/kmol]$
$T$	=The reaction temperature	$[K]$
$\beta$	=Heating rate	$[K/s]$
$T_m$	=Characteristic temperature	$[K]$

## References

- Aboulkas, A. and El-Harfi, K. "Study of the kinetics and mechanisms of thermal decomposition of Moroccan tafaya oil shale and its kerogen", *Oil Shale*, **25**, 426-443 (2008).
- Ahmad, M., Mehmood, M. A., Al-Ayed, O.S., Ye G., Luo, H., Ibrahim, M., Rashid, U. Nehdi, I. A., and Qadir, G. "Kinetic analysis and pyrolytic behavior of Para grass (*Urochloa mutica*) for its bioenergy potential", *Bioresour. Technol.*, **224**, 708-713 (2017).
- Agrawal, R. "Kinetics of reactions involved in pyrolysis of cellulose I. The reaction model", *Can. J. Chem. Eng.*, **66**, 403-412. (1988.)
- Al-Ayed, O. "Study of the kinetics and mechanisms of thermal decomposition of Ellajjun oil shale", *Academia.edu*, (2011).
- Anca-Couce, A., Mehrabian, R., Scharler, R. and Oberberger, I. "Kinetic scheme of biomass pyrolysis considering secondary charring reactions", *Energy Convers. Manag.*, **87**, 687-696, (2014).
- Anca-Couce, A. "Reaction mechanisms and multi-scale modelling of lignocellulosic biomass pyrolysis", *Prog. in Energy and Combust. Sci.*, **53**, 41-79 (2016).
- Angin, D., "Effect of pyrolysis temperature and heating rate on biochar obtained from pyrolysis of safflower seed press cake", *Biores. Tech.*, **128**, 593-597 (2013).
- Antal, M. J., Varhegyi, G., and Jakab, E. "Cellulose pyrolysis kinetics: revisited", *Ind. Eng. Chem. Res.*, **37**, 1267-1275 (1998).
- Balan, V., "Current challenges in commercially producing biofuels from lignocellulosic biomass", *ISRN Biotechnol.*, **4**, 463074 (2014).
- Basu, P., "Biomass gasification and pyrolysis. Practical design and theory", *Elsevier Inc.*, (2010).
- Behrendt, F., and Neubauer, Y. M Oevermann, M., Wilmes, B., and Zober, N. "Direct Liquefaction of biomass", *Chem. Eng. Technol.*, **31**(5), 667-77 (2008).
- Bhavanam, A., and Sastry, R. "Kinetic study of solid waste pyrolysis using distributed activation energy model", *Bioresour. Technol.*, **178**, 126-131, (2015).
- Bonilla, J., Salazar, R. P., and Mayogra, M. "Kinetic triplet of Colombian sawmill wastes using thermogravimetric analysis", *Heliyon*, **5**, e02723, (2019).
- Borah, P. C. Ghosh, P., and Rao, P. G. "A review on devolatilization of coal in fluidized bed", *Int. J. Energy Res.*, **25**, 929-963, (2011).
- Bradbury, A. G. W., Sakai, Y., and Shafizadeh, F. "Kinetic model for pyrolysis of cellulose", *J. Appl. Polym. Sci.*, **23**, 3271-3280, (1979).
- Braun, R. L., and Burnham, A. K. "Analysis of chemical reaction kinetics using a distribution of activation energies and simpler models", *Energy and Fuels*, **1**, 153-161, (1987).
- Broido, A., and Nelson, M. A. "Char yield on pyrolysis of cellulose", *Combustion and Flame*, **24**, 263-268, (1975).
- Burnham, A. K., and Braun R. L. "Global kinetic analysis of complex materials", *Fuels*, **13**, 1-22 (1999)
- Cai, J. M., Jin C., and Chen Y. "Logistic distributed activation- Part 1. Derivation and numerical parametric study", *Biores. Tech.*, **102**, 1556-1561, (2011).
- Cai J. M., Yang S. Y., and Li T. "Logistic distributed activation energy model-Part 2: Application to cellulose pyrolysis", *Biores. Tech.*, **102**, 3642-3644 (2011).
- Carpenter, D., and Westover, T. L., Czernika, S., and Jablonskia, W., "Biomass feedstocks for renewable fuel production: a review of the impacts of feedstock and pretreatment on the yield and product distribution of fast pyrolysis bio-oils and vapors", *Green Chem.*, **16**, 384- 406 (2014).
- Ceylan, S., and Kazan, D. "Pyrolysis kinetics and thermal characteristics of microalgae *Nannochloropsis oculata* and *Tetraselmis* sp", *Biores. Tech.*, **187**, 1-5, (2015).
- Chandrasekaran, A. Ramachandran, S., and Subbiah, S. "Determination of kinetic parameters in the pyrolysis operation and thermal behavior of *Prosopis juliflora* using thermogravimetric analysis", *Biores. Tech.*, **233**, 413-422 (2017).
- Chen, D., Shuang, E., and Liu Lu. "Analysis of pyrolysis characteristics and kinetic of sweet sorghum bagasse and cotton stalk", *J. Therm. Anal. Calorim.*, **131**, 1899-1909, (2017).
- Chen, J., Mu, L., Jiang, B. Yin, H., Song, X., and Li, A. "TG/DSC-FTIR and Py-GC investigation on pyrolysis characteristics of petrochemical wastewater sludge", *Biores. Tech.*, **192**, 1-10, (2015).
- Chen, L., Liao, Y., Guo, Z., Cao, Y., and Ma, X. "Products distribution and generation pathways of cellulose pyrolysis", *J. of Cleaner Prod.*, **232**, 1309-1320 (2019).
- Coats, A. W., and Redfern, J. "Kinetic parameters from thermogravimetric data", *Nature*, **201**, 68-69 (1964).
- Corbetta, M., Pierucci, S., Ranzi, E., Bennadji, H., and Fisher, E. "Multistep kinetic model of biomass pyrolysis", *XXXVI Meeting of the Italian Section of the Combustion Institute*, 111-139, (2013).
- Cuoci, A., Faravelli, T., Frassoldati, A., Granata, S., Migliavacca, G., Ranzi, E., and Sommariva, S. "A general mathematical model of biomass devolatilization Note 1. Lumped kinetic models of cellulose, hemicellulose and lignin", *30<sup>th</sup> Meeting of the Ital. Sect. Combust. Inst.*, 1-6, (2007).
- Damartzis, T., Vamvuka, D., Sfakiotakis, S., and Zabaniotou, A. "Thermal degradation studies and kinetic modeling of cardoon (*Cynara cardunculus*) pyrolysis using thermogravimetric analysis (TGA)", *Biores. Tech.*, **102**, 6230-6238 (2011).
- DeGroot, W. F., and Shafizadeh, F. "Kinetics of gasification of Douglas fir and cottonweed chars by carbon dioxide", *Fuel*, **63**, 210-216 (1984).
- Demirbas, A. "Biomass and wastes: Upgrading alternative fuels", *Energy Sources*, **25**, 317-329 (2003).
- Demirbas, A. "Effect of initial moisture content on the yields of oily products from pyrolysis of biomass", *J. Anal. Appl. Pyrolysis*, **71**, 803-815 (2004).
- Demirbas, A. "Hydrocarbon from pyrolysis and hydrolysis process of biomass", *Energy Sources*, **25**, 67-75 (2003).
- Diebold, J. P. "A unified, global model for the pyrolysis of cellulose", *Biomass and Bioenergy*, **7**, 75-85, (1994).
- Doyle, C. D. "Estimating isothermal life from thermogravimetric data", *J. Appl. Polymer Sci.*, **6**, 639-642 (1962).
- Doyle, C. D. "Kinetic analysis of thermogravimetric data", *J. Appl. Polymer Sci.*, **5**, 285-292 (1961).
- Friedman, H. L. "Kinetics of thermal degradation of char-forming plastics from thermogravimetry. Application to a phenolic plastic", *J. of Poly. Sci. Part C.*, **6**, 183-195, (1960).
- Funke, A., and Ziegler, F. "Hydrothermal carbonization of biomass: a summary and discussion of chemical mechanisms for process engineering", *Biofuels Bioproducts and Biorefining*, **4**, 160-77 (2010).
- Garcia-Maraver, A., Perez-Jimenez, J., Serrano-Bernardo, F., and Zamorano, M. "Determination and comparison of combustion kinetics parameters of agriculture biomass from olive trees", *Renew. Energy*, **83**, 897-904, (2015).
- Gronli, M. G., and Melaaen, M. "Mathematical model for wood pyrolysis-comparison of experimental measurements with model predictions", *Energy and Fuels*, **14**, 791-800 (2000).
- Hameed, S., Sharma, A., Pareek, V., Wua, H., and Yua, Y., "A review on biomass pyrolysis models: Kinetic, network, and mechanistic", *Biomass and Bioenergy J.*, **123**, 104-122 (2019).

- Heydari, M., Rahman, M., and Gupta, R. "Effect of temperature, pressure, and residence time on pyrolysis of Pine in an entrained flow reactor", *Energy and Fuels*, **28**, 5144-5157 (2015).
- Hosoya, T., Kawamoto, H., and Saka, S. "Secondary reactions of lignin-derived primary tar components", *J. Anal. Appl. Pyrolysis*, **83**, 78–87 (2008).
- Hu, M., Chen, Z., Wang, S., Guo, D., Ma, C., Zhou, Y., Chen, J., Laghari, M., Fazal, S. Xiao, B. Zhang, B., and Ma, S. "Thermogravimetric kinetics of lignocellulosic biomass slow pyrolysis using distributed activation energy model, Fraser-Suzuki deconvolution, and iso-conversional method", *Energy Convers. Manag.*, **118**, 1–11 (2016).
- Hu, S., Jess, A., and Xu, M. "Kinetic study of Chinese biomass slow pyrolysis: Comparison of different kinetic models", *Fuel*, **86**, 2778-2788 (2007).
- Huang, Y. F., Chiueh, P. T., Kuan, W. H., and Lo, S. "Pyrolysis kinetics of biomass from product information", *Appl. Energy*, **110**, 1-8 (2013).
- Katarzyna, S., Barocci, P. and Fantozzi, F. "Thermogravimetric analysis and kinetic study of poplar wood pyrolysis", *Appl. Energy*, **97**, 491-497(2012).
- Islam, M. A., Asif, M., and Hameed, B. H. "Pyrolysis kinetics of raw and hydrothermally carbonized Karanj (*Pongamia pinnata*) fruit hulls via thermogravimetric analysis", *Biores. Tech.*, **179**, 227-233 (2015).
- Kawamoto, H. "Lignin pyrolysis reactions", *J. Wood Sci.*, **63**, 117-132 (2017).
- Kissinger, H. E., "Reaction kinetics in differential thermal analysis", *Anal. Chem.*, **29**, 1702–1706 (1957).
- Klass, D. L., "Biomass for Renewable Energy, Fuels, and Chemicals", *Academic Press*, **30**, 276–277 (1998).
- Kongkaew, N., Pruksakit, W., and Patumsawada, S., "Thermogravimetric kinetic analysis of the pyrolysis of rice straw", *Energy Procedia*, **79**, 663-670, (2015).
- Koufopoulos, C. A., Maschio, and A., and Lucchesi, A., "Kinetic modelling of the pyrolysis of biomass and biomass components", *Can. J. Chem. Eng.*, **67**, 75-84 (1989).
- Koufopoulos, C. A., Papayannakos, N., Maschio, G., and Lucchesi, A., "Modelling of the pyrolysis of biomass particles. Studies on kinetics, thermal and heat transfer effects", *Can. J. Chem. Eng.*, **69**, 907-915 (1991).
- Lakshmanan, C. C., and White, N. "A new distribution activation energy model using Weibull distribution for the representation of a complex kinetics", *Energy Fuels*, **8**, 1158-1167 (1994).
- Lam, K. L., Oyedun, A. O., and Hui, C. "Experimental and modelling studies of biomass pyrolysis", *Chinese J. of Chem. Eng.*, **20**, 543-550 (2012).
- Lakshmanan, C. C. and White, N. "A new distributed activation energy model using Weibull distribution for the representation of complex kinetics", *Energy and Fuels*, **8**, 1158-1167 (1994).
- Lédé, J., "Cellulose pyrolysis kinetics: An historical review on the existence and role of intermediate active cellulose", *J. Anal. Appl. Pyrolysis*, **94**, 17-32 (2012).
- Lewis, A. D., and Fletcher, T. "Prediction of sawdust pyrolysis yields from a flat-flame burning using the CPD model", *Energy Fuels*, **27**, 942-953, (2013).
- Li, D., Chen, L., Zhang, X., Ye, N., and Xing, F. "Pyrolytic characteristics and kinetic studies of three kinds of red algae", *Biomass and Bioenergy*, **35**, 1765-1772, (2011).
- Liu, H., Ahmad, M. S., Alhumade, H., Elkamel, A., and Cattolica, R. "Three pseudo-components kinetic modelling and nonlinear dynamic optimization of Rhus Typhina pyrolysis with the distributed activation energy mode", *Appl. Thermal Engineering*, **157**, 113633-113640 (2019).
- Liu, H., Wang, C., Zhao, W., Yang, S., and Hou, X. "Pyrolysis characteristics and kinetic modeling of Artemisia apiacea by thermogravimetric analysis", *J. Therm. Anal. Calorim.*, **131**, 1783-1892, (2017).
- Maria, L., Millan, R., Emiro, F., Vargas, S., and Nzihou, A. "Kinetic Analysis of tropical lignocellulosic agrowaste pyrolysis", *Bioenergy Research*, **10**, 832-845, (2017).
- Maurya, R., Ghosh, T., Saravaia, H., Paliwal, C., Ghosh, A., and Mishra, S. "Non-isothermal pyrolysis of de-oiled microalgal biomass: Kinetics and evolved gas analysis", *Biores. Tech.*, **221**, 251-261 (2016).
- McKendry, P. "Energy production from biomass (part 1): overview of biomass. *Biores. Tech.*, **83**, 37-46 (2002).
- Mehooda, M. A., Ahmad, M. S., Liu, Q., Liu, C. G., Tahir, M. H., Alqobi, A. A., Tarbiah, N. I., Alsufianie, H. M., and Gull, M. "Helianthus tuberoses as a promising feedstock for bioenergy and chemicals appraised through pyrolysis, kinetics, and TG-FTIR-MS based study", *Energy Conv. Manag.*, **194**, 37-45, (2019).
- Mehrabian, R., Scharler, R., and Obernberger, I. "Effects of pyrolysis conditions on the heating rate in biomass particles and applicability of TGA kinetic parameters in particle thermal conversion modelling", *Fuel*, **93**, 567-575 (2012).
- Meng, A., Zhou, H., Qin, L., Zhang, Y., and Li, Q. "Quantitative and kinetic TG-FTIR investigation on three kinds of biomass pyrolysis", *J. Anal. Appl. Pyrolysis.*, **104**, 28-37 (2013).
- Mishra, G., and Bhaskar, T. "Non isothermal model free kinetics for pyrolysis of rice straw", *Biores. Tech.*, **169**, 614-621 (2014).
- Mishra, R. K., and Mohanty, K. "Pyrolysis kinetics and thermal behavior of waste sawdust biomass using thermogravimetric analysis", *Biores. Tech.*, **251**, 63-74 (2018).
- Mitu, M. Islam, Md. A., Rahman, Md. S., Feroz, S. M., Mollick, A. S., and Kabir, E. "Pyrolysis kinetic study on waste particle residue from particle board industry", *J. Indian Acad Wood Sci.*, **16**, 58-66 (2019).
- Mohan, D., Pittmann, C.V., and Steele, P. "Pyrolysis of wood/biomass for bio oil: a critical review", *Energy Fuels*, **20**, 848-889 (2006).
- Newalkar, G., Lisa, K., D'Amico, A D., Sievers, C., and Agrawal, P. "Effect of temperature, pressure, and residence time on pyrolysis of pine in an engrained flow reactor", *Ener. and Fuels*, **28**, 5144-5157 (2014).
- Niksa, S. "Predicting detailed products of secondary pyrolysis of diverse forms of biomass", *Proce. Combust. Inst.*, **28**, 2727-2733, (2000).
- Niksa, S. "Rapid coal devolatilization as an equilibrium flash distillation", *AIChE J.*, **34**, 79-82 (1987).
- Papari, S., and Hawboldt, K. "A review on the pyrolysis of woody biomass to bio-oil: focus on kinetic models", *Renew. Sustain. Energy Rev.*, **52**, 1580-1595, (2015).
- Patra, T. K., and Sheth, P. "Biomass gasification models for downdraft gasifiers: A state of the art review", *Renew. Sustain. Energy Rev.*, **50**, 583-593 (2015).
- Patwardhan, P. R., Satrio, J. A., Brown, R. C., and Shanks, B. H. "Product distribution from fast pyrolysis of glucose-based carbohydrates", *J. Anal. Appl. Pyrolysis.*, **86**, 323–330 (2009).
- Prakash, N., and Karunanithi, T. "Kinetic modeling in biomass pyrolysis – a review", *J. Appl. Sci. Res.*, **4**, 1627-1636 (2008).
- Que, H., Dong, Y., Guo, H., Lu, X., Zhu, X., Zhang, Y., and Gu, X. "Pyrolytic kinetics of steam exploded lignin by TG/DTG analysis", *Wood Res.*, **5**, 871-878, (2019).

- Ranzi, E., Cuoci, A., Faravelli, T., Frassoldati, A., Migliavacca, G., Pierucci, S., and Sommariva, S., "Chemical kinetics of biomass pyrolysis", *Energy Fuels*, **22**, 4292-4300 (2008).
- Roslee, A. N., and Munajat, N. "Comparative study on the pyrolysis behavior and kinetics of two macroalgae biomass (*Gracilaria changii* and *Gelidium pusillum*) by thermogravimetric analysis", 4<sup>th</sup> *International Conference on Mechanical Engineering Research (ICMER)*, Malaysia (2017).
- Scott, D. S., Piskorz, J., and Radlein, D. "Liquid products from the continuous flash pyrolysis of biomass", *Ind. Eng. Chem. Process Des. Dev.*, **24**, 581-588, (1985).
- Serio, M. A. "A comprehensive model of biomass pyrolysis", Final report by Advance Fuel Research Inc, 1-47, (1997).
- Sharma, A., Pareek, V., and Zhang, D. "Biomass pyrolysis- A review of modelling, process parameters and catalytic studies", *Renew. Sustain. Energy Rev.*, **50**, 1081-1096 (2015).
- Sheng, C., and Azevedo, J. "Modeling biomass devolatilization using the chemical percolation devolatilization model for the main components", *Proce. Combust. Inst.*, **29**, 407-414, (2002).
- Sheth, P. N., and Babu, B. "Kinetic modelling of the pyrolysis of biomass", *Env. Eng.*, **4**, 453-458 (2006).
- Simone, B., and Michael, S. "Biochemical conversion processes of lignocellulosic biomass to fuels and chemicals- a review", *CHIMIA Int. J. for Chem.*, **69**, 572- 581 (2015).
- Solomon, P. R., Hamblen, D. G. Serio, M. A., Yu, Z., and Charpenay, S. "A characterization method and model for predicting coal conversion behavior", *Fuel*, **72**, 469 488 (1993).
- Solomon, P. R., and King, H. "Tar evolution from coal and model polymers: theory and experiments", *Fuel*, **63**, 1302-1311 (1983).
- Soria-Verdugo, A., Garcia-Gutierrez, L., Blanco-Cano, L., Garcia-Hernando, N., and Ruiz-Rivas, U. "Evaluating the accuracy of the distributed activation energy model for biomass devolatilization curves obtained at high heating rates", *Energy Convers. Manag.*, **86**, 1045-1049, (2014).
- Turner, F., and Mann, U. "Kinetic investigation of wood pyrolysis", *Ind. Eng. Chem. Process. Des. Dev.*, **20**, 482-488, (1981).
- Tripathi, M., Sahu, J. N., and Ganesan, P. "Effect of process parameters on production of biochar from biomass waste through pyrolysis: A review", *Renew. Sustain. Energy Rev.*, **55**, 467-481 (2016).
- Varhegyi, G., Jakab, E., and Anatal, M. "Is the Briodo-Shafizadeh model for cellulose pyrolysis true? ", *Energy and Fuels*, **8**, 1345-1352 (1994).
- Vasques Mendon, A. R., Guelli U., De Souza, S. M. A., Balle, J. A. B., and Ulson de Souza, A. "Thermogravimetric analysis and kinetic study of pyrolysis and combustion of residual textile sludge", *J. Therm Anal Calorim.*, **121**, 807-814 (2015).
- Vinu, R., and Broadbelt, L. "Unravelling reaction pathways and specifying reaction kinetics for complex systems", *Annu. Rev. Chem. Biomol. Eng.*, **3**, 29-54 (2012).
- Wadhvani, R., Sutherland, D., Moinuddin, K.A., and Joseph, P. "Kinetics of pyrolysis of litter materials from pine and eucalyptus forests", *J. Therm Anal Calorim.*, **130**, 2035-2046 (2017).
- Wan, K., Wang, Z., He, Y., Xia, J., Zhou, Z., Zhou, J., and Cen, K. "Experimental and modeling study of pyrolysis of coal, biomass and blended coal-biomass particles", *Fuel*, **139**, 356-364 (2015).
- White, J. E., Catallo, W. J., and Legendre, B. "Biomass pyrolysis kinetics: a comparative critical review with relevant agricultural residue case studies", *J. Anal. Appl. Pyrolysis.*, **91**, 1-33 (2011).
- William, J., and Tarutis Jr. "A mean-variance approach for describing organic matter decomposition", *J. Theor. Biol.*, **168**, 13-18 (1994).
- Wu, Z., Wang, S., Zhao, J., Chen, L., and Meng, H. "Thermal behavior and char structure evolution of bituminous coal blends with edible fungi residue during co-pyrolysis", *Energy and Fuels*, **28**, 1792-1801 (2014).
- Xu, B., Kuang, D., Liu, F., Lu, W., Goroncy, A. K., He, T., Gasem, K., and Fan, M. "Characterization of Powder River basin coal pyrolysis with cost-effective and environmentally friendly composite Na-Fe catalyst in a thermogravimetric analyzer and a fixed reactor", *Intl. J. of Hydrogen Energy*, **43**, 6918-6935 (2018).
- Yang, H., Yan, R., Chen, H., Lee, D. H., and Zheng, C. "Characteristics of hemicellulose, cellulose and lignin pyrolysis", *Fuel*, **86**, 1781-1788 (2007).
- Yaun, T., Tahmasebi, A., and Yu, J. "Comparative study on pyrolysis of lignocellulosic and algal biomass using a thermogravimetric and a fixed bed reactor", *Biores. Tech.*, **175**, 333-341 (2015).
- Ye, N., Li, D., Chen, L., Zhang, X., and Xu, D. "Comparative studies of the pyrolytic and kinetic characteristics of Maize straw and the seaweed *Ulva pertusa*", *PLoS ONE*, **5**, e12641:1-6, (2010).
- Zhang, Q, Chang, J, Wang, T, and Xu, Y. "Review of biomass pyrolysis oil properties and upgrading research", *Energy Conver. Mange.*, **48**, 87-92 (2007).
- Zou, S., Wu, Y. Yang, M., Li, C., and Tong, J. "Pyrolysis characteristics and kinetics of the marine microalgae *Dunaliella tertiolecta* using thermogravimetric analyzer", *Biores. Tech.*, **101**, 359-365 (2010).